Formation of atypical podosomes in extravillous trophoblasts regulates extracellular matrix degradation

Running title: Atypical podosome formation in trophoblasts

Anand Patel and Philip R Dash*

School of Biological Sciences, Hopkins Building, University of Reading, Whiteknights Campus, Reading, Berkshire, RG6 6UB, UK.

*Corresponding author:

Dr Philip R Dash

School of Biological Sciences

Hopkins Building

University of Reading

Whiteknights

Reading

Berkshire, RG6 6UB

UK

Tel (0044) 0118 378 7400

p.r.dash@reading.ac.uk

Abstract

Throughout pregnancy the cytotrophoblast, the stem cell of the placenta, gives rise to the differentiated forms of trophoblasts. The two main cell lineages are the syncytiotrophoblast and the invading extravillous trophoblast. A successful pregnancy requires extravillous trophoblasts to migrate and invade through the decidua and then remodel the maternal spiral arteries. Many invasive cells use specialised cellular structures called invadopodia or podosomes in order to degrade extracellular matrix. Despite being highly invasive cells, the presence of invadapodia or podosomes has not previously been investigated in trophoblasts. In this study these structures have been identified and characterised in extravillous trophoblasts. The role of specialised invasive structures in trophoblasts in the degradation of extracellular matrix was compared with well characterised podosomes and invadopodia in other invasive cells and the trophoblast specific structures were characterized by using a sensitive matrix degradation assay which enabled visualisation of the structures and their dynamics. We show trophoblasts form actin rich protrusive structures which have the ability to degrade the extracellular matrix during invasion. The degradation ability and dynamics of the structures closely resemble podosomes, but have unique characteristics that have not previously been described in other cell types. The composition of these structures does not conform to the classic podosome structure, with no distinct ring of plaque proteins such as paxillin or vinculin. In addition, trophoblast podosomes protrude more deeply into extracellular matrix than established podosomes, resembling invadopodia in this regard. We also show several significant pathways such as Src kinase, MAPK kinase and PKC along with MMP-2 and 9 as key regulators of extracellular matrix degradation activity in trophoblasts, while podosome activity was regulated by the rigidity of the extracellular matrix.

Keywords - Trophoblasts / invadosome / invasion / extracellular matrix / podosome / pre-eclampsia

Introduction

Trophoblasts are cells that differentiate from the blastocyst during early pregnancy and migrate into the uterus, anchoring the developing embryo and connecting with the maternal blood supply. The migration of trophoblast cells is an essential part of early pregnancy and placental development, yet the molecular mechanisms and signalling pathways which regulate this process are largely unknown.. An invasive sub-population of trophoblasts - the extravillous trophoblasts - migrate as far as the myometrium, remodelling the maternal blood vessels and adapting them for the higher blood flow requirement of the fetus later in pregnancy. The importance of trophoblast migration is highlighted by the fact that complications of pregnancy such as pre-eclampsia are commonly associated with poor trophoblast invasion (Goldman-Wohl and Yagel, 2002, Kaufmann, et al., 2003). Pre-eclampsia affects 5-8% of pregnancies, is characterized by hypertension and proteinuria and is a major cause of maternal death (HMSO, 1994). Offspring from pregnancies complicated by pre-eclampsia may also suffer long-term health problems, including an increased incidence of hypertension, heart disease and diabetes and mothers whose pregnancies are complicated by pre-eclampsia have a significantly increased risk of cardiovascular disease later in life including hypertension, ischaemic heart disease and stroke (Barker, 1997).

Many studies have investigated the regulation of trophoblast invasion and subsequent spiral artery remodelling (Cartwright, et al., 2002, Cartwright and Wareing, 2006) however no attempt has been made to determine if trophoblasts employ specialised invasive structures such as invadopodia or podosomes, which are collectively known as invadosomes. Specialised invasive structures have been reported in cancer and monocytic cells in 2-D and more recently 3-D studies have demonstrated the importance of these structures in tissue invasion (Buccione, et al., 2009, Linder, 2007). Invadosomes are actin rich membrane protrusions, similar in principle to filopodia, that protrude into and degrade the extracellular matrix (ECM). The two types of invadosome, invadopodia and podosomes, share many similarities in structural components but there are key differences in several aspects. Firstly, podosomes are usually found in monocytic cells, endothelial cells and smooth muscle cells whereas invadopodia are found in

invasive cancer cells (Buccione, et al., 2009, Buccione, et al., 2004, Linder, et al., 1999, Weaver, 2006). They can be distinguished by the size of the structure and their abundance. Podosomes are usually small shallow structures, 1µm in diameter and 0.4µm in height while invadopodia are much larger structures with dimensions as large as 8µm by 5µm. Podosomes are usually more abundant in cells than invadopodia, with cells typically forming a minimum of 20 podosomes (with over a hundred per cell reported in some cases), whereas the number of invadopodia per cell is usually between one and ten. The dynamics of each structure is another factor to distinguish between them. Invadopodia are more stable structures and can persist for over an hour whereas podosomes are highly dynamic and have a turnover of only a few minutes (Chan, et al., 2009, Destaing, et al., 2003, Linder, 2007).

Both invadopodia and podosomes are able to degrade the ECM, however the extent of degradation differs between the two structures (Bowden, et al., 2006, Burgstaller and Gimona, 2005). Degradation by an invadopodium is much deeper into the matrix than the shallow degradation by podosomes. This is thought to be due to the different life spans of invadopodia and podosomes. The recruitment of proteolytic enzymes such as matrix metalloproteinases (MMPs) and serine proteinases to invadosomes are required for the ECM degradation. MMP-2, MMP-9 and MT1-MMP have been extensively implicated in degradation of ECM by invadopodia and podosomes as with trophoblast cell invasion (Nakahara, et al., 1997, Redondo-Munoz, et al., 2006, Sato, et al., 1997, Whitley and Cartwright).

In this study we have identified and characterised the invasive structures that are formed by extravillous trophoblasts. With the use of confocal microscopy we have visualised these structures and the nature of ECM degradation and conclude that extravillous trophoblasts use atypical podosomes to degrade extracellular matrix and that these podosomes have properties that appear to be unique to trophoblasts. We have also identified key regulators of the structures and examined their ability to degrade the extracellular matrix.

Results

Trophoblasts exhibit matrix degrading actin rich protrusions

To investigate if trophoblast cells form invadosome-like structures that have been reported in other cell types, extravillous trophoblast derived HTR8-svneo (HTR8) cells were initially cultured on plastic and actin rich structures were stained using fluorescently labelled phalloidin and visualised (Fig. 1A) using confocal microscopy. Podosome like structures were observed on the ventral surface of these cells. The trophoblast cells were subsequently plated on AlexaFluor-546 fluorescently labelled 0.2% gelatin for 16 hours to visualise if these invasive protrusions were capable of penetrating and degrading the matrix. Fig. 1B shows structures which were composed of cortactin that were capable of invading completely through the matrix. We also found trophoblast cells are able to completely degrade the matrix over longer time periods (48 hours) (Fig. 1C) during which the cells migrate across the surface of the gelatin.

Increasing matrix density induces greater degradation

Trophoblasts were seeded on 0.2%, 0.5% and 1% concentrations of gelatin and the degrading activity compared. Degrading activity was assessed in untreated conditions and invasive podosomes were witnessed in all concentrations of gelatin. A significant difference in the level of degradation was observed when comparing the higher gelatin concentrations to the 0.2% gelatin concentration. Fig. 2A and B clearly show the difference in matrix degradation levels, in particular the area of degradation between trophoblasts grown on 0.2% (Fig. 2A) and 1% (Fig. 2B) over the same incubation period. A clear increasing trend was observed in area and intensity of degradation as the concentration increased. However, the percentage of degrading cells had no significant differences as the lowest concentration of gelatin had almost 100% of cells degrading the matrix (Fig. 2C).

Characterisation of invasive structures in trophoblast cells results in atypical podosomes

Cell-types which are known to display invadopodia and podosomes were compared to trophoblast cells. The breast cancer cell line, MDA-MB-231 for invadopodia and the macrophage cell line, IC-21 was chosen as a model for podosomes (Fig. 3A and B respectively). The degrading activity of these cells was compared to the degrading activity of trophoblasts, which was found to be similar to the behaviour of IC-21 cells than the MDA-MB-231 cells. The total degraded area was significantly higher (IC-21, $P < 0.05$; MDA-MB-231, $P < 0.01$) when compared to trophoblasts. However, the degrading intensity showed a significant difference between trophoblasts and MDA-MB-231 ($P < 0.05$), but no significant difference between trophoblasts and IC-21 cells. The data also shows significantly higher percentage of trophoblasts actively degrading the matrix compared to the IC-21 cells ($P < 0.05$). Using Cortactin, an established invadosome marker, we were able to study the turnover rates of the invasive structures in trophoblasts. As shown in Fig. 3D, the dynamics of the cortactin rich structures (invadosome) in trophoblasts highlighted by the arrowheads have a relatively high assembly/disassembly rate which is similar to the dynamics of podosomes (2-12 minutes).

Regulation of matrix degradation by trophoblasts

Nitric oxide has been shown to regulate trophoblast migration and invasion, in particular through inducible nitric oxide synthase (iNOS) (Harris, et al., 2008). Inhibition of iNOS with 1400W and of all three NOS isoforms with L-NAME showed no reduction in matrix degrading activity. Phosphatidylinositol 3-kinase (PI3-K) inhibition (using LY294002) also showed no significant reduction in the matrix degrading activity of the cells (Fig. 4A). However, using a soluble guanylate cyclase inhibitor (NS2028) to block NO mediated cGMP production significantly reduced matrix degradation as did the use of a Src Kinase inhibitor (Src Kinase Inhibitor I, Merck Biosciences), a Mitogen-activated protein kinase kinase (MAPKK) inhibitor (PD98059) and a Protein Kinase C (PKC) inhibitor (Bisindolylmaleimide I). These inhibitors also showed similar reductions in the percentage ECM

degrading intensity (Fig. 4B). However, analysis for the number of degrading cells showed only cGMP, Src and MAPKK inhibition to have a significant effect (Fig. 4C) although the effects were smaller (approximately 25% reduction) compared to the approximately 50% reduction observed in Fig. 4A and B.

Trophoblast podosomes display no colocalisation with paxillin or vinculin

Trophoblasts were stained for the plaque proteins paxillin and vinculin (vinculin not shown) which have been shown to be structural components of podosomes. Images were analysed for colocalisation of these plaque proteins with the actin rich structures. Fig. 5A shows a representative cytofluorogram and an overall analysis revealed a Pearson's coefficient of 0.06 indicating poor colocalisation between paxillin and actin in the trophoblast podosomes suggesting that they have an atypical structure. Colocalisation analysis of actin and vinculin also showed similar a Pearson's coefficient of 0.05. Fig. 5B also shows no clear distinct ring structure of the plaque proteins around the actin rich core in trophoblasts which has been reported in classic podosomes and invadopodia. However, our data may indicate that faint regions of plaque proteins are present in the core actin rich region.

Matrix degradation by trophoblast podosomes requires MMP activity

We postulated that matrix degradation by the trophoblast podosomes may require MMP activity. Using specific inhibitors to both MMP-2 and MMP-9 a significant reduction in matrix degrading ability of the cells was observed. However, the atypical invasive podosomes were still present (Fig. 6B). Both the MMP-2 and MMP-9 inhibitors showed a similar ability to reduce the degrading activity of the trophoblast podosomes (Fig. 6C) but did not inhibit their ability to form the invasive structures. Furthermore, inhibition of degrading activity by the general MMP inhibitor BB-94 was even greater than the MMP-2 and MMP-9 inhibitors (Fig. 6C) and also did not limit the podosome formation (data not shown). The percentage of cells actively degrading showed the greatest decrease following treatment with BB-94 when compared to the MMP-2 and MMP-9 inhibited cells.

Discussion

During early pregnancy trophoblasts invade the decidua and migrate towards the spiral arteries. In order to reach their final destination they need to degrade extracellular matrices (Kam, et al., 1999). It has been known for some time that invasive cells such as cancer and monocytic cells use specialised structures known as invadosomes (invadopodia or podosomes) to degrade the ECM, however these structures have not yet been investigated in trophoblasts and the role they may play in their invasion to the maternal spiral arteries. In this study we report the first observation of these structures in trophoblast cells. We demonstrate that the composition of these structures may not follow the typical invadosome structure (Linder, 2009) and possess features that may be unique to trophoblasts. Finally we also show that the matrix density/rigidity can influence the extent of invasion/degradation by trophoblasts.

The invasive nature of trophoblasts is partly due to its ability to secrete MMPs and several MMPs have been shown to be secreted by trophoblasts during invasion (Behrendtsen, et al., 1992, Harris, et al., 2010). Recently, monocytic and cancer cells have been shown to produce actin rich protrusions which colocalise with matrix degradation and may be sites of MMP activity (Buccione, et al., 2009, Linder, 2007). Consistent with actin, cortactin, an actin binding protein localises in the periphery of cell structures such as invadopodia and podosomes (Baldassarre, et al., 2003). These protrusions can be subdivided into either podosomes (present in monocytic cells) or invadopodia (present in invasive cancer cells) and each type of structure has distinctive characteristics. Podosomes, for example, are typically small (0.5-1 μm in diameter), numerous (20-200 per cell) with a short half-life and producing only shallow matrix degradation while invadopodia are much larger structures (8 μm in diameter) that are less abundant in cells (less than 10 per cell) have a much longer half-life and are capable of much deeper and more extensive matrix degradation (Linder, 2009).

Similar actin rich structures were found in trophoblast cells cultured either on plastic or on a gelatin surface. In trophoblasts these structure share many similar features with podosomes in that they are relatively small with a typical diameter of less than 1 μm (Fig.5B) and are present in large numbers within the cell (more than 20 per cell). Despite their superficial similarity with classical podosomes, these structures in trophoblast cells are capable of penetrating more deeply through the matrix than has been reported with podosomes (Fig. 1B) and in this regard are more similar to invadopodia. We also found that trophoblasts are capable of extensive matrix degradation as actively migrating cells produced matrix degradation over a wide area.

The density of gelatin concentration regulates the degradation ability of trophoblasts. We show that increasing the concentration of the gelatin matrix trophoblasts become more invasive by possessing an increased ability to degrade the matrix. Significant increases in total area and degrading intensity was observed. Cells grown on 1% gelatin also degraded a bigger surface area than their cell surface area. This data supports Alexander *et al*'s study on invadopodia on increasing gelatin concentration matrices (Alexander, et al., 2008). A few studies have now implicated a role for integrins in the signalling process during mechanosensing where signals are passed through integrins (Mueller, et al., 1999) (Alexander, et al., 2008). Increasing the concentration of gelatin also increases the number of integrin ligands which can further increase ECM-ligand signalling. This would suggest a possible role for integrins in the regulation of the podosome-like structures in trophoblasts and this will be the subject of further studies.

To further understand the degradation levels and dynamics and to fully characterize the type of structures that were being formed by trophoblasts we compared the degradation levels/activity in trophoblasts to cells which classically form either invadopodia or podosomes (Chan, et al., 2009, Destaing, et al., 2003). Comparing the depth of invasion of the structures through extracellular matrix shows that the trophoblast structures more closely resemble invadopodia present in MDA-MB-231 invasive breast cancer cells than podosomes with their shallower protrusion.. The difference in depth of invasion through the matrix can clearly be seen between the two typical forming structures in Fig. 3. When this is compared to the depth

in Fig. 1B, the depth of invasion by the trophoblast invadosome most closely resembles that of invadopodia. However, the area of degradation and intensity of degradation are more similar to the podosomes found in the IC-21 macrophage cells. We found the trophoblast structures to be highly dynamic with a half-life of only a few minutes which is more similar to podosomes (Destaing, et al., 2003, Linder, 2009) than invadopodia. The highly dynamic structures observed in trophoblast cells also correlates more closely with the type of degradation observed with podosome-dependent degradation. It therefore appears as if these invasive structures in trophoblasts could be considered to be atypical podosomes in that they share many features of podosomes but also share with invadopodia that ability to penetrate deeply into the extracellular matrix.

To investigate regulators of the atypical structures, known factors of trophoblast invasion, such as nitric oxide, cGMP, PI3-K and MAPKK were investigated (Harris, et al., 2008, LaMarca, et al., 2008). Previous studies have reported nitric oxide synthase isoforms may regulate trophoblast invasion through the S-nitrosylation of MMP-9 (Harris, et al., 2008). PI3-Kinase and mitogen-activated protein kinases (MAPK) have also been shown to regulate trophoblast motility. Other major pathways such as Src and PKC which have shown to be regulators of invadosomes in other cell types (Destaing, et al., 2011, Kelley, et al., 2010) have yet to be studied in trophoblasts.

Our results show that nitric oxide synthases appear to have no effect on the degrading activity of the invasive structures. However, inhibition of cGMP production did have a significant effect suggesting there is a potential role downstream of the nitric oxide (NO) pathway rather than any direct effects of NO such as *S*-nitrosylation. Previous studies have shown NO regulates trophoblast motility and invasion, however the lack of a role for NO in regulating trophoblast invadosomes suggests that trophoblast podosomes are regulated differently to the general invasion observed in previous studies (Ayling, et al., 2006, Cartwright, et al., 1999).

Src kinase and PKC which have already been well established as key regulators in invadosome formation (Destaing, et al., 2011, Kelley, et al., 2010, Xiao, et al., 2010) were also found to play a similar role on trophoblast invadosomes. Xiao *et al* showed that matrix degradation by MMP-9 is dependent on PKC activity, which supports our observation of reduced matrix degrading activity following PKC inhibition in trophoblasts. PI3-K and MAPK inhibition has been shown to reduce trophoblast motility (LaMarca, et al., 2008) yet only inhibition of MAPKK significantly reduce the matrix degrading activity in trophoblasts, with PI3 kinase having no significant effect.

We have also shown that trophoblast invadosomes do not have the classic composition of podosomes. We show that the ring structure of plaque proteins reported in other cell types is not evident in trophoblasts. Colocalisation analysis of the actin rich core with the plaque proteins paxillin and vinculin showed no correlation indicating that they are not part of the structure of the trophoblast podosomes. Not only did these proteins not colocalise but the distinct ring of plaque proteins around the outside of the podosome was not observed. However in some cases a faint, but not distinct, ring structure was observed indicating that the role of these plaque proteins may be different in trophoblasts. In monocytic cells podosomes are known to assemble regardless of the matrix substrate they are grown on but other cell types have shown to be matrix specific for podosome formation (Sabri, et al., 2006). Calle *et al* have showed different integrins can be responsible for the formation of these protrusive structures, depending on the cell type (Calle, et al., 2006). It is possible that the lack of the classical podosome structure may be a consequence of the matrix properties and that different matrices may produce a more classical podosome structure in trophoblasts. However, we have cultured trophoblasts on other surfaces such as fibronectin and not observed the appearance of the classical podosome structure (data not shown). In addition since the trophoblast podosomes are capable of degrading matrix it suggests that the classical podosome structure involving plaque proteins is not required for their function in trophoblasts. Further studies will be required to identify the composition of trophoblast podosomes.

Metalloproteinases (MMPs) have been reported in trophoblasts and in the remodelling of the maternal spiral arteries (Harris, et al., 2008, Harris, et al., 2010, Isaka, et al., 2003). We show that MMP-2, MMP-9 and a pan-MMP inhibitor significantly reduce the degradation of matrix by trophoblasts. The MMP-2 and MMP-9 inhibitors had a similar effect on the level of matrix degradation which is supported by Isaka *et* al's study of MMP-2 being the key regulator in matrix degradation. Using the MMP-2 and MMP-9 inhibitors in combination had no additional effect which is to be expected if MMP-9 is activated downstream of MMP-2 (Isaka, et al., 2003). Interestingly, a further reduction in matrix degradation was observed using the pan-MMP inhibitor BB-94 indicating a role for other MMP's in the degradation process. Membrane bound proteinases such as MT1-MMP have been reported in invadosomes and trophoblast invadosomes could possibly include these (Artym, et al., 2006). The remaining percentage of degraded matrix in the presence of BB-94 could possibly due to serine proteinases which have been observed in invadopodia however they have not been studied in podosomes (Artym, et al., 2006).

Poor invasion of trophoblasts are thought to lead to such conditions as pre-eclampsia yet many of the steps involved in trophoblast invasion are poorly understood. The data presented here provides new insights into the mechanisms through which trophoblasts can degrade the extracellular matrix, a key early step in the invasion process. In particular we have shown that trophoblasts form atypical podosomes during invasion which degrade extracellular matrix through the use of MMPs such as MMP-2 and MMP-9.

Materials and Methods

Cell culture

HTR-8/SVneo cells (kindly provided by Prof. Charles H. Graham, Queen's University, Kingston, Ontario, Canada) and MDA-MB-231 breast cancer cells were cultured in RPMI and DMEM respectively with the addition of 10% FBS, 2mM L-Glutamine and antibiotics. IC-21 macrophage derived cells were cultured in RPMI 1640 with 1 mM sodium pyruvate (Invitrogen, Paisley, UK), 1x non-essential amino acids (Invitrogen), 0.029 mM 2-mercaptoethanol (Invitrogen), 10% FBS and antibiotics. IC-21 cells were detached with Versene (Invitrogen).

Antibodies and inhibitors

Monoclonal anti-Cortactin (clone 4F11) and Monoclonal anti-Vinculin, (clone VIIF9) were purchased from Millipore. Monoclonal anti-Paxillin (clone Y113) was purchased from Abcam (Cambridge, UK). AlexaFluor-647 anti-mouse, AlexaFluor-647 anti-rabbit and AlexaFluor-488 Phalloidin for F-actin staining were from Invitrogen. L-NAME (a general NOS inhibitor), 1400W (an iNOS selective inhibitor) and NS202 (a soluble guanylate cyclase inhibitor), were purchased from Enzo Life Sciences. Src Inhibitor-1, a PI3 kinase inhibitor (LY294002), a MAPKK inhibitor (PD98059), a PKC inhibitor (BisindolylmaleimideI) , an MMP-2 Inhibitor (MMP Inhibitor III (2-((Isopropoxy)-(1,1′-biphenyl-4-ylsulfonyl)-amino))-N-hydroxyacetamide) , MMP-9 Inhibitor I and the general MMP inhibitor BB-94 (Batimastat) were purchased from Merck. MMP-2 Inhibitor III exhibits good specificity over MMP-9 and MMP-3 with an IC_{50} = 0.2 and 4.5 µM, respectively and shows no effect on MMP-1 and MMP-7 with IC_{50}>50µM values. MMP-9 Inhibitor I has shown to inhibit MMP-1 (IC_{50} = 1.05 µM) and MMP-13 (IC_{50} = 113 nM) only at much higher concentrations than have been used in this study.

Fluorescent matrix degradation assay and immunofluorescence

AlexaFluor 546-conjugated gelatin was prepared using the AlexaFluor 546 protein labelling kit according to the manufacturer's instructions (Invitrogen). Matrix degradation assays were performed using an adapted protocol as previously described by Artym *et al (Artym, et al., 2006).* Briefly, µ-Dishes (Thistle Scientific, Glasgow, UK) were coated with 50 µg/mL Poly-D-lysine for 20mins at room temperature, followed by PBS washes and were then fixed with 4% paraformaldehyde for 15 minutes followed by extensive PBS washes. Then, 100µL of gelatin matrix (0.2% gelatin and 0.2% Alexa Fluor 546 labelled gelatin at an 8:1 ratio) was added to the dish and incubated for 10 minutes at room temperature. After washing with PBS, cells were plated and cultured (if required) in the presence of the relevant inhibitor on the matrix for 5 hours in the case of MDA-MB-231 cells or for 16 hours for HTR8/SVneo and IC-21 cells before fixation. The cells were fixed and permeabilised with 4% Paraformaldehyde and 0.2% Triton X-100 respectively for 10 minutes each, washed with PBS and actin was visualised by staining with Alexa Flour-488 Phalloidin (Invitrogen) 1:100 in PBS for 15 minutes followed by washes with PBS. Cortactin, Vinculin and Paxillin staining was visualised by initially incubating the cells with the relevant antibody 1:100 in 2% goat serum for one hour followed by incubating with a secondary antibody, Alexa Flour 647 (Invitrogen), 1:100 in 2% goat serum. Images were subsequently analysed using Photoshop CS5 Extended (Adobe, San Jose, CA).

Podosome dynamics

HTR8/SVneo cells were transfected with mCherry-Cortactin (kindly provided by Dr Matthew Oser, Albert Einstein College of Medicine, New York, NY) using FuGENE 6 transfection reagent (Roche) at a ratio of 3:1. 24 hours post transfection the media was replaced and the dynamics of invadosomes were analysed by live cell confocal microscopy. Cortactin has been considered an accepted adapter protein to identify invadosomes. Accumulation of dense regions of cortactin was defined as an invadosome and its lifetime was analysed. This was performed by observing the structures persistent/turnover rate by

counting the time elapsed between the first and last frame in which an individual invadosome was observed.

Confocal fluorescence microscopy

Confocal images were collected using a Leica TCS-SP2 AOBS-DMIRE2 inverted confocal microscope with a 63x/1.4 oil objective. Z-stack images were taken every 0.3 µM and 3D cross sections were performed using Leica confocal analysis software.

Quantification of matrix degradation

Random cells were chosen and to quantify the area and the intensity of degradation, Adobe Photoshop CS5 Extended (Adobe, San Jose, CA) was used. Initially, the cell area was selected using the magic wand tool. The magnetic lasso tool was used to select the area of degradation and average fluorescence intensity within the degraded region. The background fluorescence intensity was obtained by inversely selecting the outlined degraded region. A minimum of 60 cells were chosen at random from at least three independent experiments carried out on separate days. All measurements shown are the mean ± SEM. The depth of the invadosome protrusion was quantified using side projections of confocal z-stack data followed by measuring the length of each invadosome with the straight line measurement tool in ImageJ.

Colocalisation analysis

Regions of interest were drawn around podosomes and Pearson's correlations and the cytofluorogram were calculated and produced using Volocity software (Massachusetts, US). A minimum of five podosomes per image from 30 images were analysed from three independent experiments carried out on separate days for both paxillin and vinculin colocalisation with actin.

Statistical analysis

Prism 5 software (GraphPad Software, La Jolla, CA) was used to perform tests for statistical significance. For statistical comparison, a one-way analysis of variance (ANOVA) followed by a Tukey post-hoc test was used with *P < 0.05, **P < 0.01 and ***P < 0.001 considered significant.

Acknowledgements

We thank E.Louise Trayhorn for helpful discussions relating to this work. This work was supported by the British Heart Foundation, London, UK (FS/08/056)

References

Alexander N.R., Branch K.M., Parekh A., Clark E.S., Iwueke I.C., Guelcher S.A. and Weaver A.M., 2008. Extracellular matrix rigidity promotes invadopodia activity. *Curr Biol*. 18, 1295-1299.

Artym V.V., Zhang Y., Seillier-Moiseiwitsch F., Yamada K.M. and Mueller S.C., 2006. Dynamic interactions of cortactin and membrane type 1 matrix metalloproteinase at invadopodia: defining the stages of invadopodia formation and function. *Cancer Res*. 66, 3034-3043.

Ayling L.J., Whitley G.S., Aplin J.D. and Cartwright J.E., 2006. Dimethylarginine dimethylaminohydrolase (DDAH) regulates trophoblast invasion and motility through effects on nitric oxide. *Hum Reprod*. 21, 2530-2537.

Baldassarre M., Pompeo A., Beznoussenko G., Castaldi C., Cortellino, S., McNiven M.A., Luini A. and Buccione R., 2003. Dynamin participates in focal extracellular matrix degradation by invasive cells. *Mol Biol Cell*. 14, 1074-1084.

Barker, D.J., 1997. The long-term outcome of retarded fetal growth. *Clinical Obstetrics & Gynecology*. 40, 853-863.

Behrendtsen, O., Alexander C.M. and Werb Z., 1992. Metalloproteinases mediate extracellular matrix degradation by cells from mouse blastocyst outgrowths. *Development*. 114, 447-456.

Bowden E.T., Onikoyi E., Slack R., Myoui A., Yoneda T., Yamada K.M. and Mueller S.C., 2006. Co-localization of cortactin and phosphotyrosine identifies active invadopodia in human breast cancer cells. *Exp Cell Res*. 312, 1240-1253.

Buccione R., Caldieri G. and Ayala I., 2009. Invadopodia: specialized tumor cell structures for the focal degradation of the extracellular matrix. *Cancer Metastasis Rev*. 28, 137-149.

Buccione R., Orth J.D. and McNiven M.A., 2004. Foot and mouth: podosomes, invadopodia and circular dorsal ruffles. *Nat Rev Mol Cell Biol*. 5, 647-657.

Burgstaller G. and Gimona M., 2005. Podosome-mediated matrix resorption and cell motility in vascular smooth muscle cells. *Am J Physiol Heart Circ Physiol*. 288, H3001-3005.

Calle Y., Burns S., Thrasher A.J. and Jones, G.E., 2006 The leukocyte podosome. *Eur J Cell Biol*. **85,** 151-157.

Cartwright J.E., Holden D.P. and Whitley G.S., 1999. Hepatocyte growth factor regulates human trophoblast motility and invasion: a role for nitric oxide. *Br J Pharmacol*. 128, 181-189.

Cartwright J.E., Kenny L.C., Dash P.R., Crocker I.P., Aplin J.D., Baker P.N. and Whitley G.S., 2002 Trophoblast invasion of spiral arteries: a novel in vitro model. *Placenta*. 23, 232-235.

Cartwright J.E. and Wareing M., 2006. An in vitro model of trophoblast invasion of spiral arteries. *Methods Mol Med*. 122, 59-74.

Chan K.T., Cortesio C.L. and Huttenlocher A., 2009. FAK alters invadopodia and focal adhesion composition and dynamics to regulate breast cancer invasion. *J Cell Biol*. 185, 357-370.

Destaing O., Block M.R., Planus E. and Albiges-Rizo C., 2011. Invadosome regulation by adhesion signaling. *Curr Opin Cell Biol*. 23, 597-606.

Destaing O., Saltel F, Geminard J.C., Jurdic P. and Bard F., 2003. Podosomes display actin turnover and dynamic self-organization in osteoclasts expressing actin-green fluorescent protein. *Mol Biol Cell*. 14, 407-416.

Goldman-Wohl D. and Yagel S., 2002. Regulation of trophoblast invasion: from normal implantation to pre-eclampsia. *Mol Cell Endocrinol*. 187, 233-238.

Harris, L.K., McCormick J., Cartwright J.E., Whitley G.S. and Dash P.R., 2008. S-nitrosylation of proteins at the leading edge of migrating trophoblasts by inducible nitric oxide synthase promotes trophoblast invasion. *Exp Cell Res*. **314,** 1765-1776.

Harris L.K., Smith S.D., Keogh R.J., Jones R.L., Baker P.N., Knofler M., Cartwright J.E., Whitley G.S. and Aplin J.D., 2010. Trophoblast- and vascular smooth muscle cell-derived MMP-12 mediates elastolysis during uterine spiral artery remodeling. *Am J Pathol*. 177, 2103-2115.

Isaka K., Usuda S., Ito H., Sagawa Y., Nakamura H., Nishi H., Suzuki Y., Li Y.F. and Takayama M., 2003. Expression and activity of matrix metalloproteinase 2 and 9 in human trophoblasts. *Placenta*. 24, 53-64.

Kam E.P., Gardner L., Loke Y.W. and King A., 1999 The role of trophoblast in the physiological change in decidual spiral arteries. *Hum Reprod.* 14, 2131-2138.

Kaufmann P., Black S. and Huppertz B., 2003. Endovascular trophoblast invasion: implications for the pathogenesis of intrauterine growth retardation and preeclampsia. *Biol Reprod.* 69, 1-7.

Kelley L.C., Ammer A.G., Hayes K.E., Martin K.H., Machida K., Jia L., Mayer B.J. and Weed S.A., 2010 Oncogenic Src requires a wild-type counterpart to regulate invadopodia maturation. *J Cell Sci*. 123, 3923-3932.

LaMarca H.L., Dash P.R., Vishnuthevan K., Harvey E., Sullivan D.E., Morris C.A. and Whitley G.S., 2008. Epidermal growth factor-stimulated extravillous cytotrophoblast motility is mediated by the activation of PI3-K, Akt and both p38 and p42/44 mitogen-activated protein kinases. *Hum Reprod*. 23, 1733-1741.

Linder S., 2007. The matrix corroded: podosomes and invadopodia in extracellular matrix degradation. *Trends Cell Biol*. 17, 107-117.

Linder S., 2009. Invadosomes at a glance. *J Cell Sci*. 122, 3009-3013.

Linder S., Nelson D., Weiss M. and Aepfelbacher M., 1999. Wiskott-Aldrich syndrome protein regulates podosomes in primary human macrophages. *Proc Natl Acad Sci U S A*. 96, 9648-9653.

Mueller S.C., Ghersi G., Akiyama S.K., Sang Q.X., Howard L., Pineiro-Sanchez M., Nakahara H., Yeh Y. and Chen W.T., 1999 A novel protease-docking function of integrin at invadopodia. *J Biol Chem*. 274**,** 24947-24952.

Nakahara H., Howard L., Thompson E.W., Sato H., Seiki M., Yeh Y. and Chen W.T., 1997. Transmembrane/cytoplasmic domain-mediated membrane type 1-matrix metalloprotease docking to invadopodia is required for cell invasion. *Proc Natl Acad Sci U S A*. 94, 7959-7964.

Redondo-Munoz J., Escobar-Diaz E., Samaniego R., Terol M.J., Garcia-Marco J.A. and Garcia-Pardo A., 2006. MMP-9 in B-cell chronic lymphocytic leukemia is up-regulated by alpha4beta1 integrin or CXCR4 engagement via distinct signaling pathways, localizes to podosomes, and is involved in cell invasion and migration. *Blood.* 108, 3143-3151.

Sabri S., Foudi A., Boukour S., Franc B., Charrier S., Jandrot-Perrus M., Farndale R.W., Jalil A., Blundell M.P., Cramer E.M., Louache F., Debili N., Thrasher A.J. and Vainchenker W., 2006. Deficiency in the Wiskott-Aldrich protein induces premature proplatelet formation and platelet production in the bone marrow compartment. *Blood*. 108, 134-140.

Sato T., del Carmen Ovejero M., Hou P., Heegaard A.M., Kumegawa M., Foged N.T. and Delaisse J.M., 1997. Identification of the membrane-type matrix metalloproteinase MT1-MMP in osteoclasts. *J Cell Sci*. 110 (Pt 5), 589-596.

Weaver A.M., 2006. Invadopodia: specialized cell structures for cancer invasion. *Clin Exp Metastasis*. 23, 97-105.

Whitley G.S. and Cartwright J.E., 2010. Cellular and molecular regulation of spiral artery remodelling: lessons from the cardiovascular field. *Placenta*. 31, 465-474.

Xiao H., Bai X.H., Kapus A., Lu W.Y., Mak A.S. and Liu M., 2010 The protein kinase C cascade regulates recruitment of matrix metalloprotease 9 to podosomes and its release and activation. *Mol Cell Biol*. 30, 5545-5561.

Figure legends

Figure 1

Trophoblasts form actin rich invasive protrusions which have the ability to degrade the extracellular matrix. (**A**) Trophoblast cell stained with AlexaFluor-488-Phalloidin show actin rich structures on the ventral surface of the cell when plated on plastic. When plated on fluorescently labelled gelatin (0.2% w/v), degradation of the extracellular matrix is observed (**B**) Trophoblast cell displaying similar actin rich structures as in A which are also cortactin rich (blue), similar to the composition of invadosomes. Cells were also plated on fluorescently labelled gelatin and the overlaid image of actin (green) and gelatin (red) shows that these structures were able to invade and degrade the fluorescent matrix. (**C**) Trail of

degradation by a migrating trophoblast cell through fluorescently labelled matrix. Arrow heads indicate a single actin rich protrusion. All scale bars equal to 10 µm.

Figure 2

Increased density of gelatin promotes trophoblast matrix degradation. (**A**) Typical single point degradation levels by trophoblasts on a 0.2% fluorescent gelatin matrix(**B**) Degradation of gelatin by trophoblast cells on 1% w/v gelatin is seen to be greater than in Fig. 2A (0.2% w/v gelatin) over the same incubation period. (**C**) Quantification of matrix degraded shows a significant increasing trend for degraded area and degrading intensity for trophoblast cells on increasing concentrations of gelatin. Percentage of degrading cells does not differ with trophoblast cells on 0.2% gelatin close to 100%. * $P < 0.05$, ** $P < 0.01$ and *** $P < 0.001$. Arrow heads indicate a single actin rich protrusion. All scale bars equal to 10 µm.

Figure 3

Invasive structures in trophoblast cells are more closely related to podosomes than invadopodia. (**A**) Classical invadopodia found in cancer cells (MDA-MB-231 breast cancer cells) which show large invasive actin rich structures penetrating through the gelatin. (**B**) Typical podosomes found in monocytic cells (IC-21 macrophage cells) with more numerous but more shallow actin rich structures which penetrate the gelatin. (**C**) Quantification of area of degradation, intensity of fluorescence of degradation and actively degrading cells. Degradation of the extracellular matrix by trophoblast cells resembles more closely to podosome-like degradation than invadopodia. (**D**) Invadosome dynamics of trophoblast cells transfected with mCherry-Cortactin are similar to the high assembly/disassembly rates of podosomes. Rapid dynamic cortactin rich regions (minutes compared to up to an hour for invadopodia) are illustrated with different coloured arrows for newly assembled structures. * $P < 0.05$ and ** $P < 0.01$. Arrow heads indicate actin and cortactin rich protrusions. All scale bars equal to 10 µm.

Figure 4

Regulators of extracellular matrix degradation by trophoblasts. (**A**) The degraded area was analysed and calculated as a percentage against the cell area. A significant similar reduction in the area of degradation was observed with cGMP (NS2028), Src (Src Inihibitor-1), MAPKK (PD98059) and PKC inhibition (Bisindolylmaleimide I). (**B**) Similar reduction levels of significant inhibitors in (A) were also found on the percentage of ECM degraded intensity. (**C**) Number of degrading cells was reduced with NS2028, Src Inhibitor-1 and PD98059 but not with Bisindolylmaleimide I as observed in (A) and (B). The following inhibitors were used at the respective concentrations, L-NAME (5mM), 1400W (10µM), NS2028 (5µM), Src inhibitor-1 (1µM), LY294002 (1µM), PD98059 (50 µM) and Bisindolylmaleimide I (100 nM). * $P < 0.05$, ** $P < 0.01$ and *** $P < 0.001$. All scale bars equal to 10 µm.

Figure 5

Trophoblast cell podosomes do not co-localise with adhesion plaque proteins nor do they form a distinct ring structure. (**A**) Representative images of a trophoblast cell stained for actin in green (podosomes) and paxillin in red (adhesion plaque protein). Upon co-localisation analysis with paxillin and vinculin (data not shown) average Pearson's correlations were 0.06 and 0.05 respectively. The cytofluorogram is a representative image of the analysis from the co-localisation quantification. (**B**) Close up of images from the panels highlighted in (A) in their respective images. No co-localisation or distinct ring structure was observed was individual channels or overlaid images. All scale bars for (**A**) equal to 10 µm and (**B**) equal to 1 µm

Figure 6

Inhibition of metalloproteinase's (MMPs) decreases trophoblast matrix degradation. (**A**) Typical degradation level observed by trophoblasts on fluorescently labelled gelatin matrix. (**B**) Trophoblast cells treated with the pan-MMP inhibitor, BB-94 (10 µM) shows significant reduction of degradation but nevertheless display invasive protrusions through the gelatin compared to Fig. 6A. (**C**) Inhibition of MMP

activity significantly decreases degrading ability of trophoblast cells to similar levels. BB-94 reduces the number of cells actively degrading to a greater extent than MMP-2 (50 nM) and MMP-9 (50 nM) inhibition. * $P < 0.05$, ** $P < 0.01$ and *** $P < 0.001$. Arrow heads indicate a single actin rich protrusion. All scale bars equal to 10 µm.

Figure 1

A

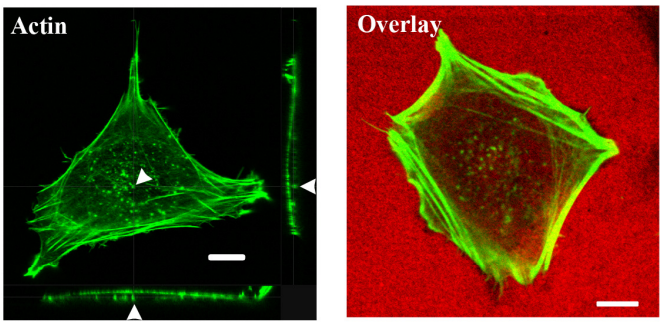
Actin
Overlay

B

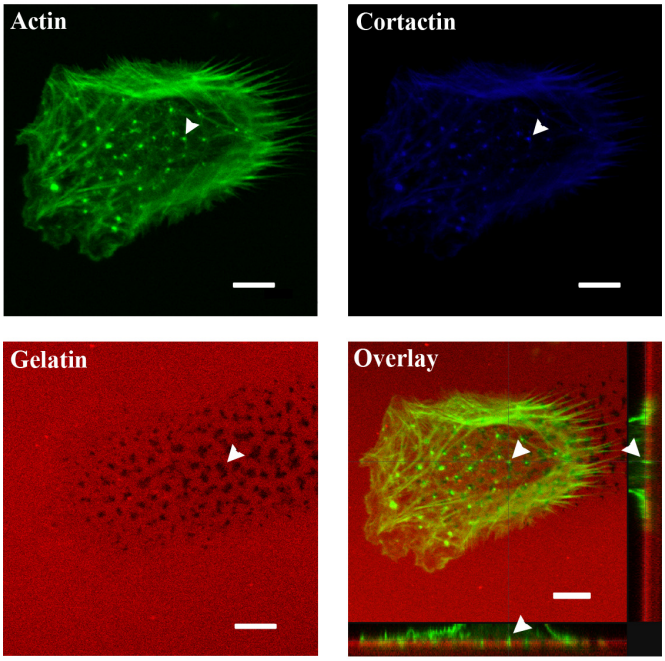
Actin
Cortactin
Gelatin
Overlay

C

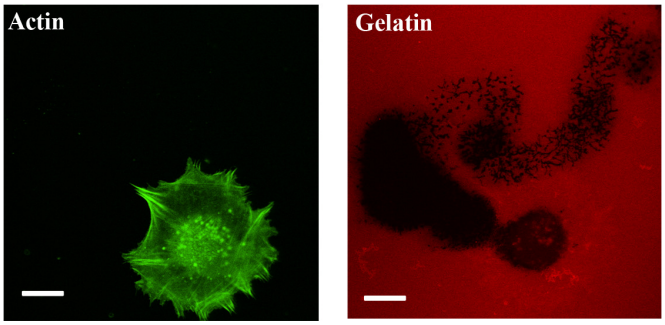
Actin
Gelatin

Figure 2

A

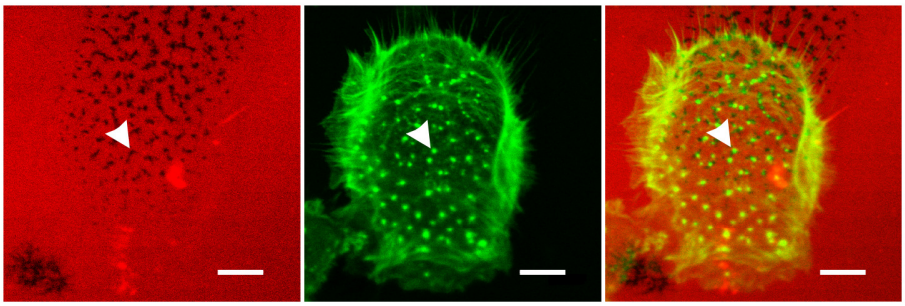

B

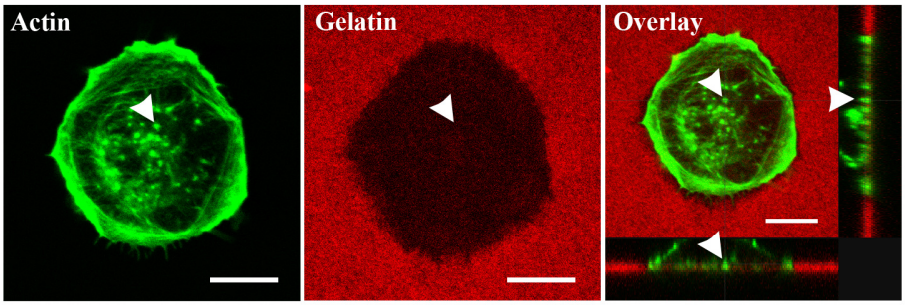
Actin
Gelatin
Overlay

C

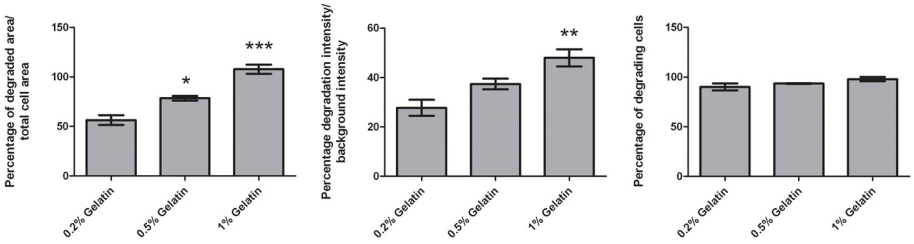
Percentage of degraded area/ total cell area
150
100
50
0
*
***
0.2% Gelatin
0.5% Gelatin
1% Gelatin
Percentage degradation intensity/ background intensity
60
40
20
0
**
0.2% Gelatin
0.5% Gelatin
1% Gelatin
Percentage of degrading cells
150
100
50
0
0.2% Gelatin
0.5% Gelatin
1% Gelatin

Figure 3

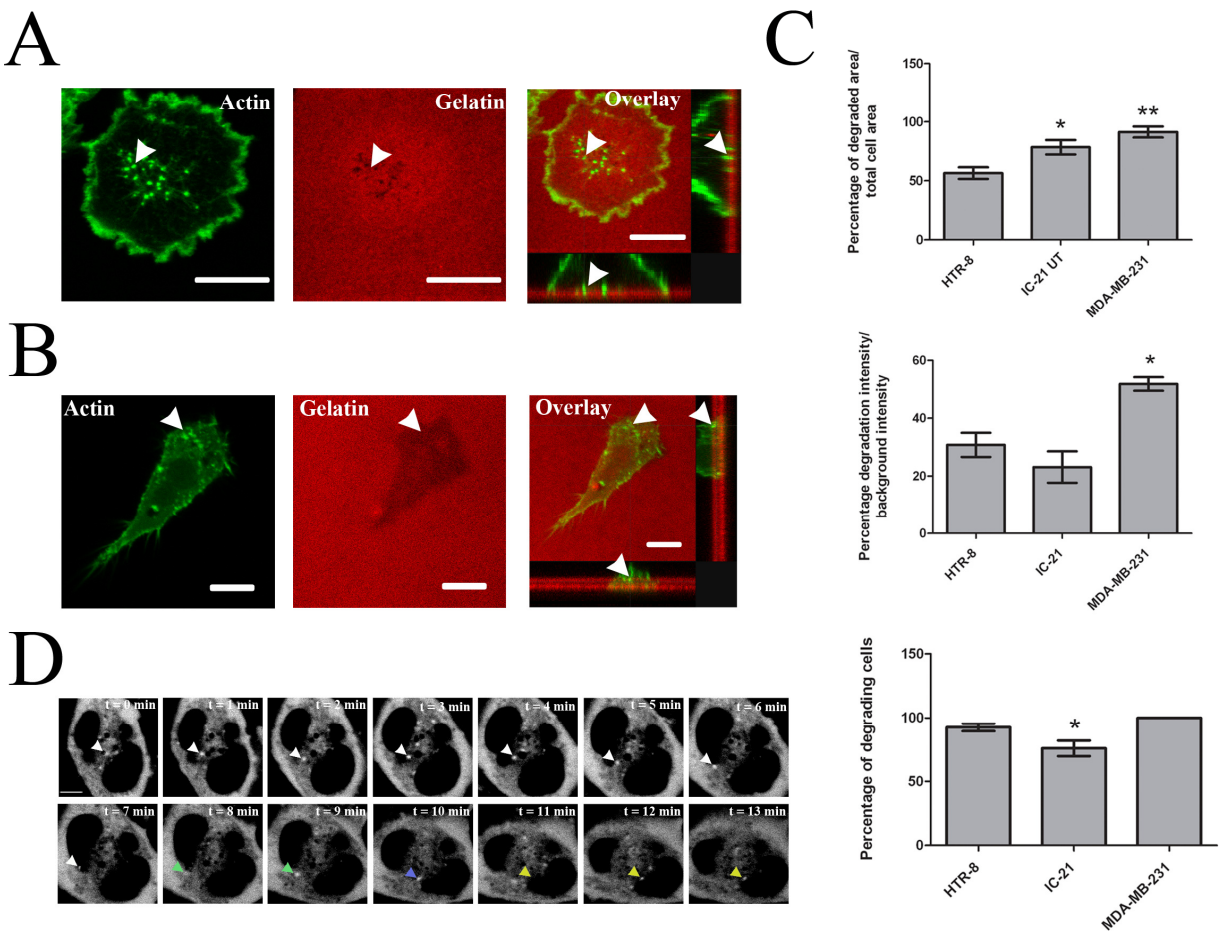

Figure 4

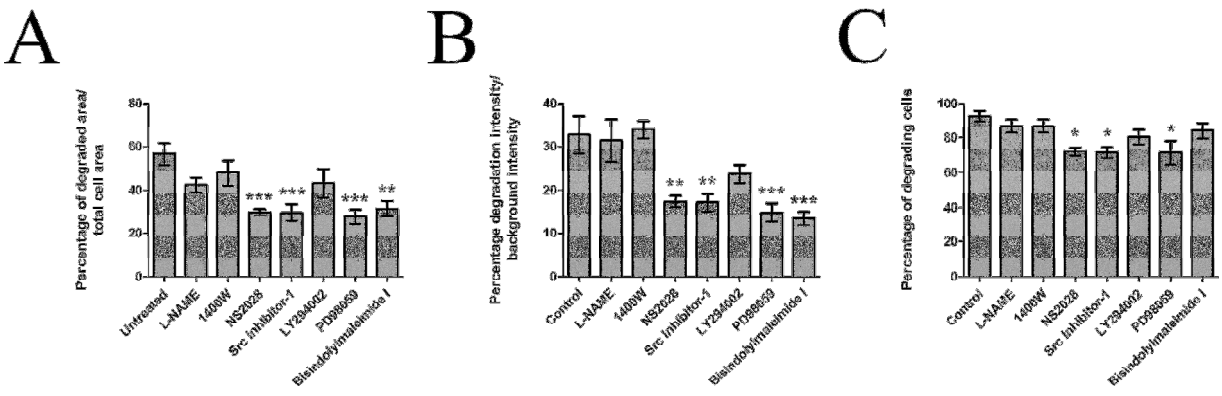

Figure 5

A

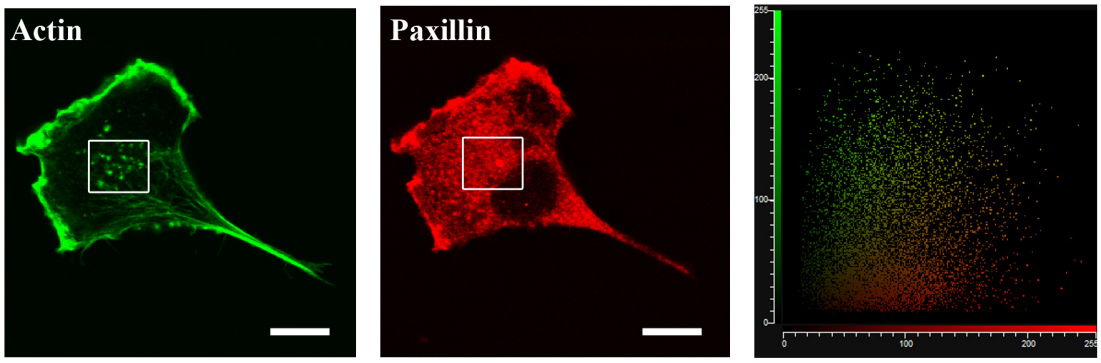
Actin
Paxillin
255
200
100
0
0
100
200
255

B

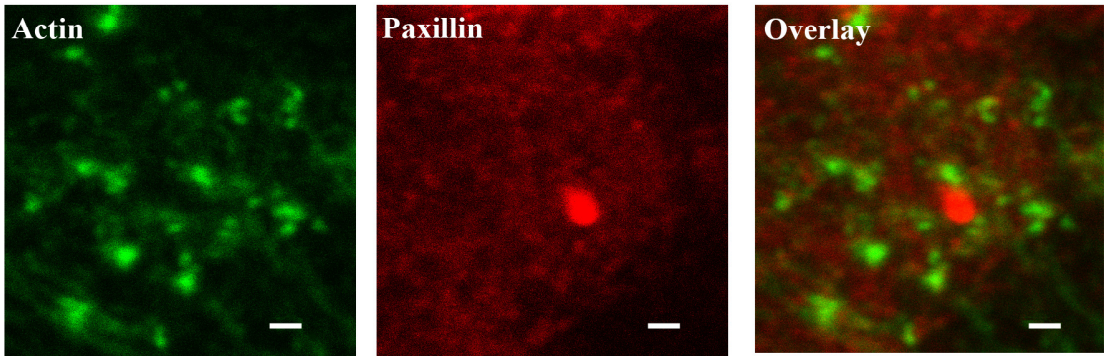
Actin
Paxillin
Overlay

Figure 6

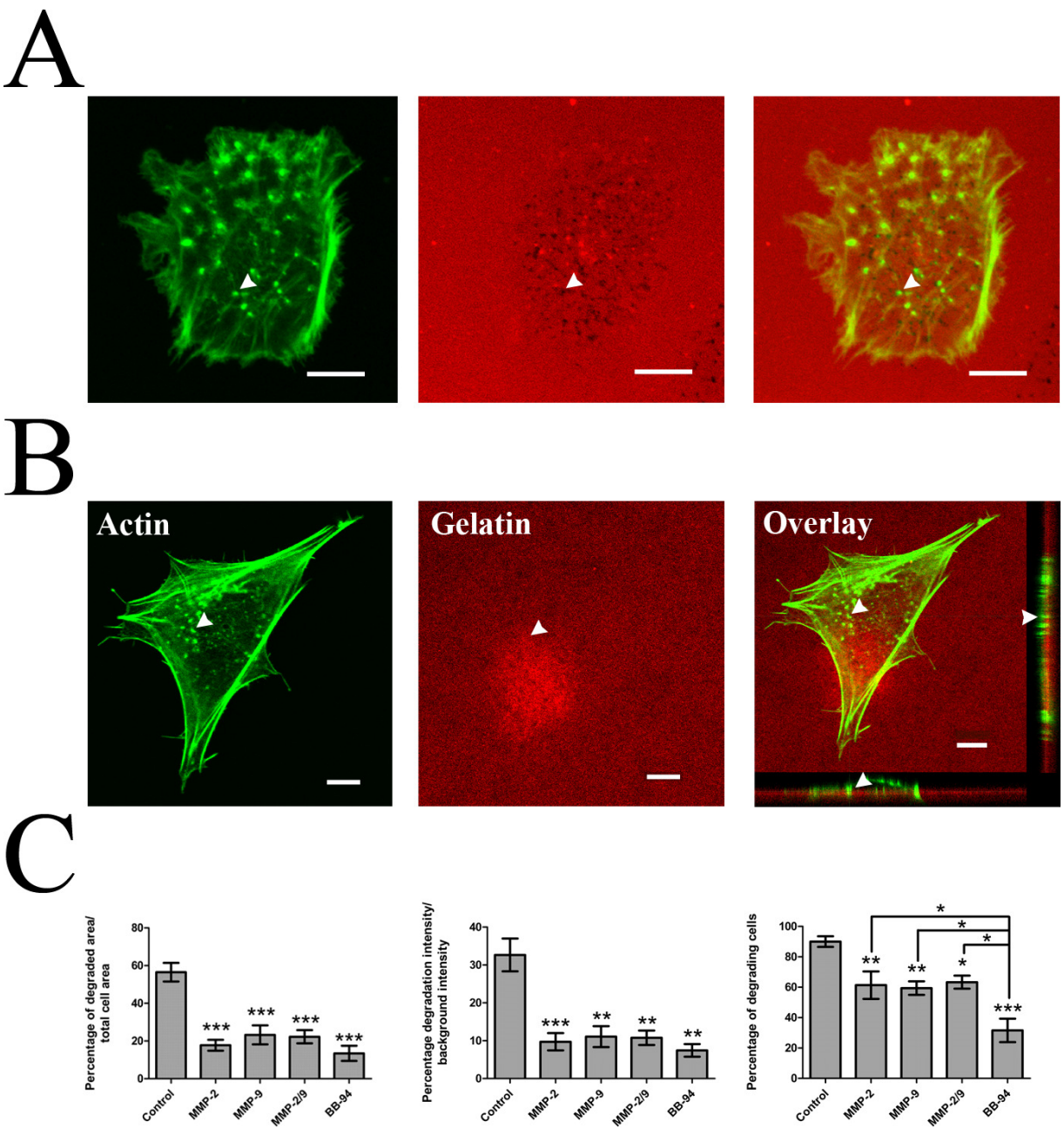
A
B
Actin
Gelatin
Overlay
C
Percentage of degraded area/ total cell area
Percentage degradation intensity/ background intensity
Percentage of degrading cells
Control
MMP-2
MMP-9
MMP-2/9
BB-94